Gold nanoparticles enhance the radiation therapy of a murine squamous cell carcinoma

2010 Phys. Med. Biol. 55 3045

(http://iopscience.iop.org/0031-9155/55/11/004)

IOP PUBLISHING PHYSICS IN MEDICINE AND BIOLOGY

Phys. Med. Biol. **55** (2010) 3045–3059 doi:10.1088/0031-9155/55/11/004

Gold nanoparticles enhance the radiation therapy of a murine squamous cell carcinoma

James F Hainfeld[1], F Avraham Dilmanian[2,3], Zhong Zhong[4], Daniel N Slatkin[1], John A Kalef-Ezra[5] and Henry M Smilowitz[6,7]

[1] Nanoprobes, Inc., Yaphank, NY 11980, USA
[2] Medical Department, Brookhaven National Laboratory, Upton, NY 11973, USA
[3] Department of Radiation Oncology, State University of New York, Stony Brook, NY 11794, USA
[4] National Synchrotron Light Source, Brookhaven National Laboratory, Upton, NY 11973, USA
[5] Medical Physics Laboratory, Medical School, University of Ioannina, Ioannina, 45110, Greece
[6] Diagnostic Imaging & Therapeutics, Cell Biology and Immunology, University of Connecticut Health Center, Farmington, CT 06030, USA

E-mail: smilowitz@nso1.uchc.edu

Received 17 September 2009, in final form 3 March 2010
Published 12 May 2010
Online at stacks.iop.org/PMB/55/3045

Abstract

The purpose of this study is to test the hypothesis that gold nanoparticle (AuNP, nanogold)-enhanced radiation therapy (nanogold radiation therapy, NRT) is efficacious when treating the radiation resistant and highly aggressive mouse head and neck squamous cell carcinoma model, SCCVII, and to identify parameters influencing the efficacy of NRT. Subcutaneous (sc) SCCVII leg tumors in mice were irradiated with x-rays at the Brookhaven National Laboratory (BNL) National Synchrotron Light Source (NSLS) with and without prior intravenous (iv) administration of AuNPs. Variables studied included radiation dose, beam energy, temporal fractionation and hyperthermia. AuNP-mediated NRT was shown to be effective for the sc SCCVII model. AuNPs were more effective at 42 Gy than at 30 Gy (both at 68 keV median beam energy) compared to controls without gold. Similarly, at 157 keV median beam energy, 50.6 Gy NRT was more effective than 44 Gy NRT. At the same radiation dose (∼42 Gy), 68 keV was more effective than 157 keV. Hyperthermia and radiation therapy (RT) were synergistic and AuNPs enhanced this synergy, thereby further reducing TCD50 s (tumor control dose 50%) and increasing long-term survivals. It is concluded that gold nanoparticles enhance the radiation therapy of a radioresistant mouse squamous cell carcinoma. The data show that radiation dose, energy and hyperthermia influence efficacy and better define the potential utility of gold nanoparticles for cancer x-ray therapy.

[7] Author to whom any correspondence should be addressed.

Introduction

Gold-based nanostructures (e.g. nanoparticles, nanocages, nanorods, nanoshells, nanotubes) are currently undergoing intensive investigation for their use in cancer diagnosis, imaging and therapy (e.g. Boisselier and Astruc 2009, Muthu and Singh 2009, Yang and Cui 2008, Skrabalak *et al* 2007, Hirsch *et al* 2006). Numerous gold nanoparticle-based applications for solid tumor therapy are under investigation including photodynamic therapy (Cheng *et al* 2008), photothermal therapy (Lal *et al* 2008), radiofrequency-mediated hyperthermia, nano-based chemotherapy (Bawarski *et al* 2008) and gold nanoparticle (AuNP, Nanogold)-enhanced radiation therapy (NRT) (Hainfeld *et al* 2008, for a recent review). Here we focus on NRT, as theoretical considerations have long suggested that heavy metals can augment the efficacy of orthovoltage x-ray therapy. In our laboratories, experiments with mice have lent credence to those predictions. Although photon-activation therapy using iodine contrast agents and compounds as well as gold sheets (Regulla *et al* 1998) and gold microparticles (Herold *et al* 2000) showed evidence of enhanced cell killing (Adams *et al* 1977, Matsudaira *et al* 1980, Nath *et al* 1990, Boudou *et al* 2005), our approach was to use small AuNPs as a method of enhancing delivery of high-Z material to tumors. The strategy was to load tumors with gold in the form of AuNPs thereby preferentially increasing radiation doses to cells near AuNPs from photoelectron and secondary electron cascades produced by high-Z ($Z = 79$) gold atoms interacting with x-rays in the 'orthovoltage' range (Roeske *et al* 2007, Cho 2005, McMahon *et al* 2008). Since nanoparticles are known to permeate leaky angiogenic endothelium via the enhanced permeability and retention (EPR) effect (Dvorak 1990, Moore *et al* 2000), some tumor specificity may be obtained even in the absence of specific targeting methods. This approach was validated using the EMT-6 mouse mammary carcinoma grown sc in the mouse thigh (Hainfeld *et al* 2004). Irradiation (26 Gy, 250 kVp x-rays) $\sim$1 min after the iv injection of 2.7 g Au kg^{-1}, 1.9 nm AuNPs, resulted in 86% long term survival ($>$1 year) compared to identical irradiation without gold which showed only 20% survival (Hainfeld *et al* 2004). To follow up this work, we tested the hypothesis that AuNPs would enhance x-ray therapy of a more radioresistant tumor and explored several parameters that might influence the efficacy of the technique including radiation dose, beam energy and hyperthermia due to the well-documented synergy of hyperthermia with x-rays (Kampinga 2006). In this study we used a cell line derived from a spontaneously arising squamous cell carcinoma (SCCVII) in a C3H/HeJ mouse (O'Malley *et al* 1997, Yang *et al* 2003). The SCCVII model is considerably more resistant to radiation (TCD50 = 55.4 Gy, Yahiro *et al* 2005) and more invasive (Nomura *et al* 2006) than the EMT-6 model (TCD50 = 37 Gy: Dilmanian *et al* 2001, 2003). In fact, the SCCVII line was developed specifically to model, in the mouse, the most therapeutically intractable squamous cell cancers encountered in and around the human head and neck (Argiris *et al* 2008).

Materials and methods

Cell culture

SCCVII cells obtained from the American Type Culture Collection (Manassas, VA) were grown on Sarstedt tissue culture flasks (Newton, NC) in DMEM-CM (GIBCO #11995) supplemented with glutamine (2 mM), Penn/Strep (100 U ml^{-1} penicillin; 100 μg ml^{-1} streptomycin), and Fungizone (0.25 μg ml^{-1}), all from Invitrogen (Grand Island, NY).

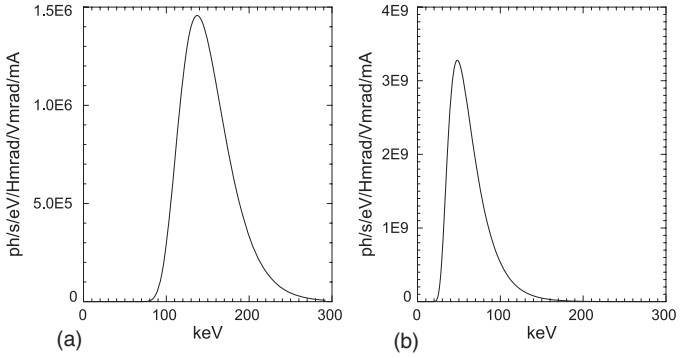

Figure 1. Spectra of the beam flux for the 157 keV and 68 keV median energy beams. The wiggler beam was filtered with 4 mm Al, 19 mm Cu and 4 mm Al, 0.25 mm Cu to produce the 157 keV (a) and 68 keV (b) median energy beams, respectively. The calculations used the code Source (Chapman *et al* 1988). The beam flux is given in units of number of photons per eV energy bandwidth per horizontal and per vertical milliradian and per mA current of the electron storage ring.

Subcutaneous tumors

Subcutaneous SCCVII tumors were initiated by injecting 200 000 cells in a total volume of 50–100 μl (50% Matrigel, Becton-Dickinson, Bedford, MA) sc in the thighs of 8–10 week old C3H/HeJ mice (Charles River, Kingston, NY), isogenic with the SCCVII tumor. Tumors were irradiated 10–11 days after implantation when they were ∼35–150 mm^3. Untreated, mice had to be euthanized when tumors reached 500 mm^3, ∼21 days (median) post-implantation.

Gold injections

Gold nanoparticles (AuNPs, Nanogold; ∼60 000 MW, 1.9 nm diameter gold core commercially available as AuroVist^{TM}, Nanoprobes, Inc., Yaphank, NY) were injected iv at 1.9 g/kg bw (bw = body weight) in 0.2 ml PBS with no apparent short- or long-term toxicity (Hainfeld *et al* 2006); irradiations were performed, as quickly thereafter as possible (∼1 min), when blood gold levels were ∼70% of their initial peak value and tumor levels were ∼7 mg Au g^{-1} (Hainfeld *et al* 2004, 2006).

Irradiations

Irradiations were performed at the X17B1 superconducting wiggler beam line of the National Synchrotron Light Source (NSLS), Brookhaven National Laboratory (Upton, NY) at a wiggler-to-mouse distance of 29 m. The unfiltered x-ray beam from the NSLS's X17 wiggler source had a median energy of 28 keV. Two different beam filtration protocols were used to produce x-ray beams of median energies in ranges relevant to NRT: one added 4 mm Si and 0.25 mm Cu yielding an emergent median beam energy of 68 keV at an average skin-entrance dose rate of ∼1000 Gy s^{-1}; the other added 4 mm Si and 19.1 mm Cu, yielding a median emergent beam energy of 157 keV but a dose rate of only 2.0 Gy s^{-1}. The energy spectra of the resultant beams are shown in figure 1. The 30 Gy, 68 keV and 30 Gy, 157 keV doses, for example, were delivered in 30 ms and 15 s, respectively. The large difference between these two dose rates (∼500-fold) resulted from the substantial beam filtration needed to produce those beams, which decreased the source beam's flux and, concomitantly, the tumor dose rate

roughly exponentially as the median energy of the x-rays emerging from successive filters increased. A number of studies indicate that low versus high dose rates produce essentially the same radiobiological results (Viani *et al* 2009, Wilkins *et al* 1998).

To measure skin-entrance dose rates from these two types of beam filtrations, two types of radiation detectors were used for the assessment of dose in water: LiF:Mg, Ti thermoluminescent dosimeters and MD55-2 radiochromic films. The dosimeters with 15 mm of Plexiglas backscattering material were positioned where the mice would be in their holder, and then irradiated during steady, vertically upward movement of the computer-controlled mouse stage through the horizontal fan-like filtered x-ray beam. Currents in the electron storage ring were recorded concomitantly. The films were read in the transmission mode using a HP Scanjet 4570c Digital Flatbed Document Scanner. The image was split into three separate images (red–green–blue) and the amount of polymer produced by irradiation and, by extension, the depth of the color change in either the red or the green image, was related to absorbed dose in water (Kalef-Ezra and Karava 2008). Dose assessments between the two dosimetric techniques typically differed by less than 5%. The large difference in the dose rates between the two beam energies used may be considered therapeutically inconsequential since both rates are several orders of magnitude above those that would allow molecular, cellular and/or tissue damage to undergo significant repair during irradiation.

The mice were positioned in a holder comprising two square, upper and lower Plexiglas plates ($1/8''$ and $1/2''$ thick, respectively) separated by 9 cm using plastic spacers at their corners. The upper plate had a central 10 mm diameter hole for the mouse leg; the lower plate held a screw to anchor the leg via dental floss loosely tied around the mouse's ankle. The lower plate was attached to a computer-controlled stage that moved the mouse vertically through the 2 mm high, 250 mm wide fan beam to irradiate a 25 mm $\times$ 25 mm square target area, which encompassed the mouse's entire tibiofibial 'thigh' down to its ankle. For each mouse, at a given electron ring current, the scanning speed of the stage was adjusted to deliver the planned nominal radiation dose to the skin overlying the targeted tissue as if it contained no gold. The starting and stopping points in the irradiation field were determined by opening and closing a computer-controlled fast shutter. Scans were implemented using a stepping motor with 12.5 μm step sizes and the scan velocities (performed at mm s^{-1} average upward-displacement speeds) were measured well within 1% accuracy. Irradiations were implemented in a single dose or in two 15 Gy dose fractions given 24 h apart, each preceded by an AuNP injection (+AuNP).

Hyperthermia

The legs of anesthetized mice containing subcutaneous SSCVII tumors were submerged in a 44 °C water bath and heated for either 15 or 20 min as indicated. Heating at 44 °C for 15 or 20 min was chosen as an effective but moderate heating protocol on the basis of a large body of previous studies (Hinkelbein *et al* 1988).

Hyperthermia plus irradiations

Legs of anesthetized mice containing subcutaneous SCCVII tumors were heated for either 12 or 17 min prior to gold injections and then heated an additional 3 min prior to irradiations performed $\sim$1 min later, when blood gold levels had already fallen to about half of their initial (peak) concentrations.

Interpretation of data

Median time to tumor volume doubling (number of days from the date of irradiation to the date tumors doubled in volume during the progressive phase of tumor growth) and the percent of long-term survivals (>200 days, but shown as 100 or 150 days in figures 2–5 since there were no changes past 150 days) were used for Wilcoxon non-parametric rank sum statistical analyses suitable for the small groups of ∼7–10 mice used (see the tables for number of mice used for each experiment) (Lentner 1982). *Ranking*: survival to 200 days post-irradiation (tumor-free) has been ranked best, followed by time to tumor doubling (the greater the time to tumor doubling the better the ranking). All progressive phase tumor growth resulted in virtual death (euthanasia) when the tumors reached 500 mm^3.

Results

Gold nanoparticles (1.9 nm) enhance the radiation therapy (42 Gy, 68 keV) of SCCVII squamous cell carcinomas

Twelve mice received 1.9 g Au kg^{-1} of 1.9 nm AuNPs ∼1 min before irradiation of subcutaneous leg tumors (42 Gy, 68 keV); 12 mice did not receive gold injections prior to irradiation. Typically tumor volumes, plotted as a function of time after irradiation (day 0), initially increased, then decreased and then increased progressively thereafter. The median time to tumor volume doubling during the phase of progressive tumor growth in mice that ultimately died was increased from 53 days (− gold) to 76 days (+ gold) (figures 2(C), (D), table 1(B). There were 67% long-term (>200 days) survivors with gold, but only 25% without gold (2.7-fold less). Using the time to tumor doubling and long-term tumor-free survival as indices of efficacy, no-gold and gold conditions were compared by the Wilcoxon two-sample rank-sum test (Lentner 1982). Nanogold radiation therapy (NRT) for the aggressive, radiation-resistant SCCVII tumor was shown to be effective, since −gold and +gold groups are significantly different at 44 Gy ($p < 0.04$). The fractions of long-term survivors in −AuNP (figure 2(C)) and +AuNP (figure 2(D)), when analyzed separately, also differ significantly ($p < 0.04$, 2-sided Z-statistics test).

X-ray dose: AuNPs are more effective at 42 Gy (68 keV) than at 30 Gy (68 keV)

The x-ray dose was reduced to 30 Gy while keeping other parameters unchanged (beam energy, amount of gold administered, etc) (figures 2(A), (B), table 1(A)). Median tumor volume doubling times in mice that ultimately died increased 18% from 45 days to 53 days (30 Gy to 42 Gy, respectively) without gold, but increased 73% from 44 to 76 days (30 Gy to 42 Gy, respectively) with gold. At 30 Gy the use of gold did not increase the number of long-term survivors (1/7 (14%)) compared to 30 Gy without AuNPs, while at 42 Gy, AuNPs increased long-term survivors from 1/7 (14%) to 8/12 (67%). Hence, tumor responses to 30 Gy in the presence or absence of AuNPs were not significantly different, but at 42 Gy tumor responses in the presence of AuNPs were significantly different from tumor responses in the absence of AuNPs (figures 2(A), (B), (C), (D), tables 1(A), (B)) ($p < 0.02$).

X-ray beam energy: AuNPs are more effective when used at 68 keV than at 157 keV

NRT using x-ray beam energies 68 keV (42 Gy) and 157 keV (44 Gy) were compared while keeping other variables constant (x-ray dose, amount of gold administered, etc). The slight difference in dose (42 or 44 Gy, <5%) occurred due to post-experiment dosimetry correction

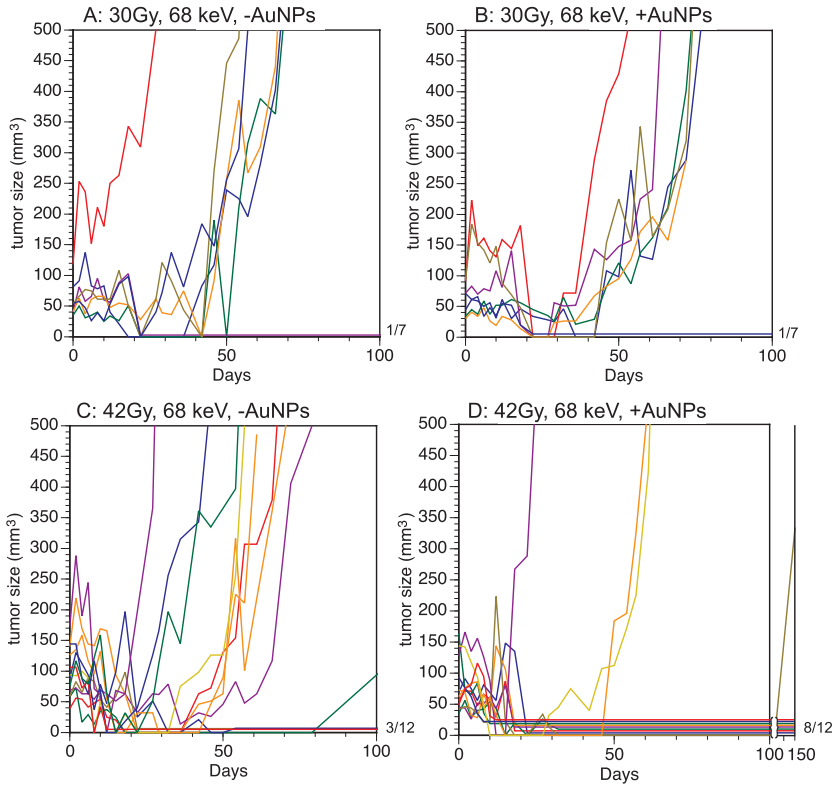

Figure 2. AuNP (1.9 nm) enhance radiation therapy of SCCVII squamous cell carcinomas more effectively at 42 Gy (68 keV) than at 30 Gy (68 keV). Mice received a single leg irradiation 10–11 days after sc implantation of 200 000 SCCVII tumor cells when the tumor volumes were 35–125 mm^3 (A) 30 Gy, 68 keV without AuNP pre-treatment, (B) 30 Gy, 68 keV 1 min after an iv injection of 1.9 nm AuNPs at 1.9 g Au kg^{-1} body weight. (C) 42 Gy, 68 keV without AuNP pre-treatment, (D) 42 Gy, 68 keV 1 min after an iv injection of 1.9 nm AuNPs at 1.9 g Au kg^{-1} body weight. Each colored line represents the tumor volume in a single mouse plotted as a function of time. Long-term survival is defined as the absence of visibly detectable/palpable tumor for >200 days. Long-term surviving mice are depicted as slightly raised above the *x*-axis for visual clarity. The fraction of long-term survivors is shown to the right of the *x*-axis. Lines that terminate before 100 days indicate mice that died or required euthanasia. No gold and AuNP-injected groups (42 Gy, 68 keV) are statistically different from one another with respect to combined median time to tumor doubling (progressive growth phase) and fraction of long-term survivors, $p < 0.041$ (Wilcoxon non-parametric statistics test) and just fraction of long-term survivors in C and D, $p < 0.041$ (2-sided *Z*-statistics test). (See tables 1(A), (B) for a summary of the results.) Only 100 days is plotted since there were no further changes at 200 days when the experiments were terminated.

and is not deemed significant since it is <5%. The results are shown in figures 2(C), (D), table 1(B) and figures 3(A), (B), table 1(C). For 68 keV (figures 2(C), (D), table 1(B)), median tumor doubling times and long-term survivors increased from 53 days (−AuNPs) to 76 days (+AuNPs) and 3/12 to 8/12, respectively. For 157 keV (figures 3(A), (B) table 1(C)), median tumor doubling times only increased from 29 days (−AuNPs) to 31 days (+AuNPs) and long-term survivors increased from 0/7 to 2/7. A comparison of the two energies revealed that median tumor doubling times were 76 days (68 keV, +AuNPs) versus 31 days (157 keV, +AuNPs) and long-term survivals were 8/12 (67%, 68 keV) versus 2/7 (29%, 157 keV),

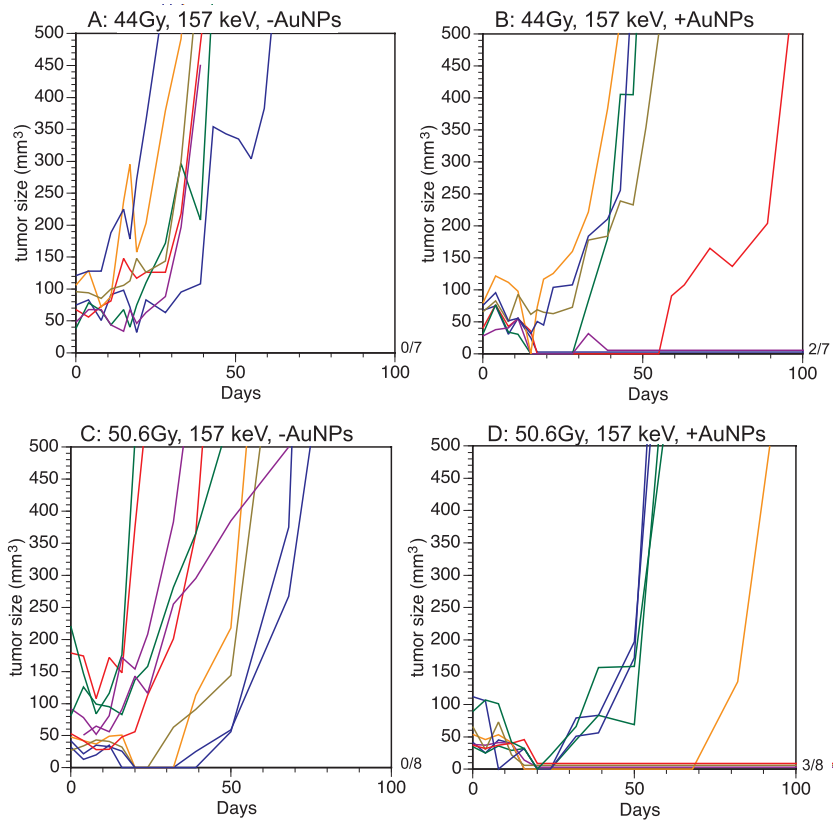

Figure 3. AuNPs are more effective when used at 68 keV than at 157 keV; AuNP NRT is more effective at 50.6 Gy, 157 keV than at 44 Gy, 157 keV. (A) 44 Gy, 157 keV, no AuNPs; (B) 44 Gy, 157 keV, plus AuNPs; (C) 50.6 Gy, 157 keV, no AuNPs; (D) 50.6 Gy, 157 keV, plus AuNPs. (See table 1(C) for a summary of the results.)

respectively (tables 1(B) and (C)). Hence tumor responses to x-ray doses of ∼43 Gy in the presence of AuNPs were significantly better at 68 keV than at 157 keV ($p < 0.05$).

AuNP-based NRT is more effective at 50.6 Gy, 157 keV than at 44 Gy, 157 keV

AuNPs enhanced radiation sensitivity at both 44 Gy (figures 3(A), (B), table 1(C)) ($p < 0.05$) and 50.6 Gy (figures 3(C), (D), table 1(C) ($p < 0.05$) but were more effective at 50.6 Gy. Without AuNPs, median time to tumor volume doubling increased only ∼7% and long-term survivors were unaffected by increasing radiation dose from 44 Gy to 50.6 Gy. However, the same dose increase in the presence of AuNPs was much more effective, increasing median tumor doubling time 58% ($p < 0.05$) and long-term survivors from 0% to 38%. At the doses used in these experiments (44 Gy or 50.6 Gy), almost all irradiated legs of long-term surviving mice in both no-gold and gold groups remained functional and continued to enable locomotion but showed some degree of partial hair loss and leg atrophy.

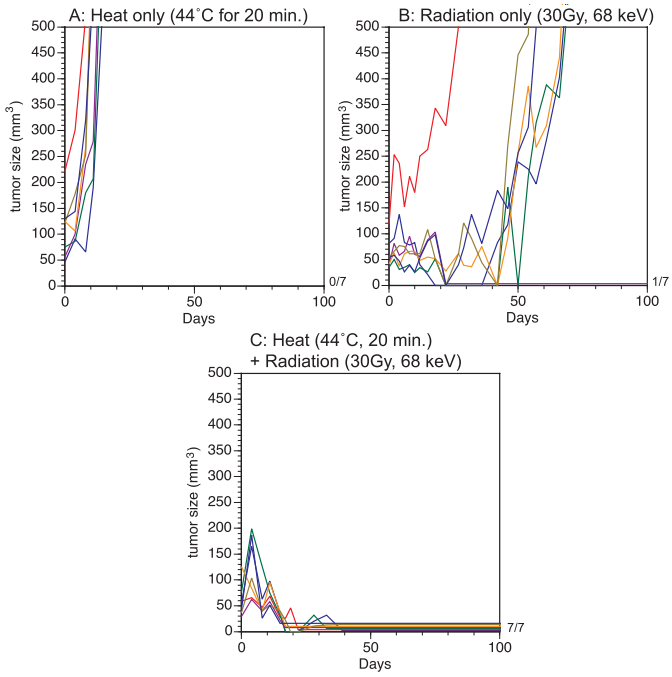

Figure 4. Synergy of hyperthermia and radiation therapy at 30 Gy, 68 keV. (A) Heat-only, 44 °C for 20 min, (B) radiation-only, 30 Gy, 68 keV, (C) heat + radiation (44 °C, 20 min + 30 Gy, 68 keV).

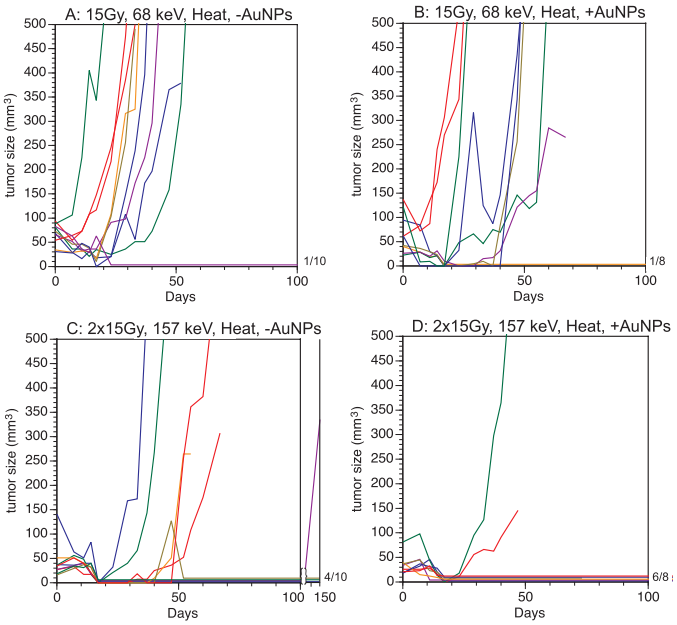

Figure 5. AuNPs increase the efficacy of hyperthermia and sub-optimal radiation therapy. (A) Heat, no AuNPs (15 Gy, 68 keV); (B) heat plus AuNPs (15 Gy, 68 keV); (C) heat, no AuNPs (2 × 15 Gy, 157 keV). Shown is one group (10 mice) of the total (20 mice). (D) Heat plus AuNPs (2 × 15 Gy, 157 keV).

Table 1. Summary of median time to tumor doubling and fraction surviving for experiments presented in figures 2 and 3.

	Median (days)	Fraction surviving	p value[a]	p value[b]
A. 30 Gy, 68 keV				
−Gold	45	1/7 (14%)		
+Gold	44	1/7 (14%)		
30 Gy, 68 keV(−Gold) versus 42 Gy, 68 keV(−Gold)			$p > 0.1$	
30 Gy, 68 keV(+Gold) versus 42 Gy, 68 keV(+Gold)			$p < 0.02$	
B. 42 Gy, 68 keV				
−Gold	53	3/12 (25%)		
+Gold	76	8/12 (67%)		
42 Gy, 68 keV(−Gold) versus 42 Gy, 68 keV(+Gold)				$p < 0.04$
C. 44 Gy, 157 keV				
−Gold	29	0/7 (0%)		
+Gold	31	2/7 (29%)		
44 Gy, 157 keV (−Gold) versus 44 Gy, 157 keV(+Gold)			$p < 0.05$	
D. 50.6 Gy, 157 keV				
−Gold	31	0/8 (0%)		
+Gold	49	3/8 (38%)		
50.6 Gy, 157 keV(−gold) versus 50.6 Gy, 157 keV(+gold)			$p < 0.05$	

[a] This p value combines time to tumor doubling and fraction surviving (Wilcoxon non-parametric statistics).
[b] Fraction surviving (2-sided Z-statistics test).

Table 2. Summary of median time to tumor doubling and fraction surviving for experiments presented in figures 4 and 5.

A. Heat only	Median (days) 7			Surviving fraction 0/7 (0%)		
	Median (days)			Surviving fraction		
	Radiation alone	Radiation + heat	Radiation + heat + gold	Radiation alone	Radiation + heat	Radiation + heat + gold
B. 1 × 15 Gy	11	25	32	0/7	1/10 (10%)	1/9 (11%)
C. 1 × 23 Gy	7.5	38.5	66	0/7	3/7 (43%)	3/6 (50%)
D. 2 × 15 Gy	ND	18	31.5	ND	8/20 (40%)	6/8 (75%)
E. 1 × 30 Gy	45		52	1/7 (14%)	7/7 (100%)	11/14 (79%)

Gold nanoparticles enhance the synergy of hyperthermia and radiation therapy at sufficiently high radiation doses

Hyperthermia (HT: 44 °C for 20 min) alone had no overtly measurable effect on SCCVII tumor growth compared to untreated tumors, as determined by sequential measurements of tumor volume, and all mice rapidly succumbed to tumor overgrowth (figure 4(A), table 2(A)). This level of HT produced no observable leg damage. Similarly, HT plus gold (without irradiation) also had no effect on SCCVII tumor growth (data not shown). RT with 30 Gy at 68 keV increased median tumor doubling times to 45 days with 1/7 long-term survival (figure 4(B),

table 2(E)). However, the combination of HT followed immediately by 30 Gy RT produced 100% long-term survival ($p < 0.001$, figure 4(C), table 2(E)) and produced no observable leg damage. HT at 44 °C for 20 min 24 h prior to RT was less effective than the same HT implemented immediately prior to RT; 57% of mice were cured of their tumors and the median time to tumor doubling for those tumors that did recur was 59 days (data not shown). This is consistent with published findings that heating 2 days before or after RT did not enhance RT while heating at the time of RT was effective (Kinuya *et al* 2000).

For lower doses of radiation with or without heating, an effect of AuNPs could be seen. If a single dose of 15 Gy (68 keV) was used, median time to tumor doubling was increased by heating (HT: 44 °C for 15 min) from 11 days to 25 days and further increased by HT and gold to 32 days, but no increase in long-term survival was observed (figures 5(A), (B); table 2(B)). Two 15 Gy (157 keV) doses separated by 3 days (temporally fractionated RT) resulted in 40% long-term survival when combined with HT (44 °C for 15 min given each time) but rose to 75% long-term survival when combined with HT and AuNPs (given iv injected 1 min prior to each irradiation) (figures 5(C), (D); table 2(D)). A single 23 Gy, 68 keV dose was more effective than a single 15 Gy, 68 keV dose (tables 2(B), (C)). Using 23 Gy alone, 23 Gy plus HT (44 °C for 15 min), and 23 Gy plus HT plus gold (all 68 keV), median tumor doubling time increased from 7.5 to 38.5 to 66 days and long-term survival similarly increased from 0% to 43% to 50%, respectively. Hence, our data suggest that AuNPs are most effective when combined with HT and RT in the order: 2×15 Gy $>$ 23 Gy $>$ 15 Gy, i.e. the less the x-ray dose, the less was the AuNP synergy with HT and RT. No observable leg damage was produced by any of the treatments involving HT, with or without these irradiations.

Discussion

NRT (Nanogold Radiation Therapy), using AuNPs is shown herein to significantly enhance the efficacy of RT for the highly aggressive (Nomura *et al* 2006), radiation-resistant SCCVII squamous cell carcinoma head and neck mouse tumor model (Yang *et al* 2003, Yahiro *et al* 2005). This result is likely to have clinical applicability (Argiris *et al* 2008). Although current radiation therapy is largely megavoltage based, a number of studies have shown that othovoltage radiotherapy (<500 keV) is feasible for some human tumors (McMahon *et al* 2008). For example Rose *et al* 1999 performed a phase I clinical study in which a modified CT scanner was used to irradiate a brain tumor after infusion of iodinated x-ray contrast media while another brain tumor (control) lay completely outside the treated volume. Further, while current radiation therapy is largely fractionated, there is a large literature on the use of radiosurgery (i.e. single dose, Serizawa 2009). Perhaps both theoretical considerations showing the feasibility of gold nanoparticle enhancement (Cho 2005, Roeske *et al* 2007, McMahon *et al* 2008, Montenegro *et al* 2009, Zhang *et al* 2009, Cho *et al* 2009), *in vitro* studies (Ito *et al* 2009, Roa *et al* 2009, Zheng and Sanche 2009, Rahman *et al* 2009, Kong *et al* 2008) and direct demonstrations of efficacy in animals such as ours will provide the impetus to develop the use of orthovoltage radiation therapy for those patients who would benefit from it.

The proportional efficacy of AuNP enhancement of RT for SCCVII has been found to be greater at higher x-ray doses—both at 68 keV and at 157 keV. A possible explanation is that the sigmoidal dose-response curve for x-ray therapy is such that at low doses, the enhancement provided by AuNPs still does not reach the part of that curve in which increasing dose provides increased survival. Thus, at either very low or very high radiation doses one should not expect any significant therapeutic gain from gold.

The presence of AuNPs locally increases the energy transferred from photons to electrons, primarily by photoelectric interactions. The kerma (kinetic energy released in matter) enhancement ratio due to gold, KER, is given by equation (1):

$$\mathrm{KER} = \left[\sum_i (P_i \times \mu_{en,\,w,\,i} \times \rho_{w,i} \times E_i) + \sum_i (P_i \times \mu_{en,\,Au,\,i} \times E_i)\right] \Big/ \sum_i (P_i \times \mu_{en,\,w,\,i} \times \rho_{w,i} \times E_i) \quad (1)$$

where i is the index of the spectral energy bin, P_i is the spectral yield for the bin i, $\mu_{en,w,i}$ and $\mu_{en,\,Au,\,i}$ are the mass energy absorption coefficients of gold and water for the energy bin i, $\rho_{w,i}$ and and $\rho_{Au,i}$ are the densities of water and that of gold inside the tumor, respectively, and Ei is the mean photon energy in bin i. Examples for the values of $\mu_{en,w,i}$ and $\mu_{en,\,Au,\,i}$ used in this equation are, for the 68 keV, 0.030 $\mathrm{cm^2\ g^{-1}}$ and 2.7 $\mathrm{cm^2\ g^{-1}}$, respectively, and for the 157 keV energy bin, 0.028 $\mathrm{cm^2\ g^{-1}}$ and 0.94 $\mathrm{cm^2\ g^{-1}}$, respectively. The electrons ejected from the nanoparticles (primarily photoelectrons and electrons ejected during the rearrangement of the electrons in the gold atoms) deposit most of their kinetic energy in the surrounding tissue, thus increasing the dose absorbed in cells close to the nanoparticles.

For both energy spectra used in the studies reported here (68 and 157 keV median energies), the photoelectric cross sections in gold are larger than those of Compton or coherent scattering by orders of magnitude. Considering the 157 keV beam, the fluorescent yield from the gold K shell is 96.4% and the probability of an Auger electron emission is therefore only 3.6% (Browne and Firestone 1986). Therefore, after ejection of an electron from the K shell by a photon of energy larger than 80.725 keV (the electron binding energy of the K shell, which is the main interaction mechanism with the 157 keV beam), most of the fluorescent photon energy is deposited at a large distance from the AuNP, due to the small attenuation coefficient of the characteristic x-ray in water, $\sim$0.2 $\mathrm{cm^{-1}}$. A 66.4 keV to 80.7 keV photon (depending on the transition, $\mathrm{K}\alpha_{\mathrm{av}} = 68.2$) corresponds to a mean free path of $\sim$35 mm, an order of magnitude larger than the dimensions of the tumor. The remaining energy becomes kinetic energy of the photoelectron, 76.3 keV in the case of an initial photon 157 keV in energy. This photoelectron has a high probability of depositing its energy in the tumor due to its range of $\sim$85 μm in water. Therefore, for 157 keV, only about half of the photon energy ($76/157 = 48\%$) is deposited inside the tumor.

For 68 keV photons, the most probable interaction with the gold is again photoelectron emission. The energy of the ejected electron depends on the L subshell (L1, 11.56 keV; L2, 13.27 keV; and L3, 13.88 keV), and for an average L shell energy of $\sim$13 keV, the photoelectron will have a mean energy of 55 keV (68 keV–13 keV). The photoelectron therefore acquires $\sim$81% of the photon energy (55/68), and deposits all of its kinetic energy within the tumor since its range is up to $\sim$40 μm. The L shell gold fluorescent yield is 76.1% (L1 10.7%, L2 33.4%, L3 32.0%, Browne and Firestone 1986). The remaining energy can be given to either a characteristic x-ray of energy of the order of 10 keV ($\mathrm{L}\alpha_{\mathrm{a1}} = 9.7$ keV), with a mean free path of $\sim$1.3 mm, or to one or more Auger electrons with ranges not exceeding $\sim$2 μm. These distances are within the tumor volume. Therefore, for 68 keV, almost 100% of the gold-absorbed photon energy is deposited inside the tumor.

Assuming a uniform gold distribution, the energy deposited as a result of the interaction of x-rays with AuNPs is anticipated to be quite uniform. More specifically, the energy is deposited by electrons, which are primarily photoelectrons and Auger electrons. The initial energy of most of these electrons, 20 to 80 keV, is such that their range in water is $\sim$8.6 to 98 μm, i.e. about 400–5000 times longer than the mean distance between neighboring AuNPs in tumors loaded uniformly with 7 mg $\mathrm{g^{-1}}$ AuNPs (which then have a mean interparticle spacing

of ∼21 nm). Their attenuation inside the 1.9 nm AuNPs is anticipated to be negligible since the corresponding range in gold is ∼1 to 10 microns. Under this uniform dose-distribution assumption, according to equation (1) above, a tissue loaded with 7 mg Au ml^{-1} that is irradiated with 68 keV and 157 keV x-ray beams increases the absorbed energy to the tissue by 88% and 24% relative to tissues without AuNPs respectively. The increased biological efficacy of the 68 keV beam, relative to that of the 157 keV beam found in the present study, is therefore consistent with theoretical predictions.

In previous work, Regulla *et al* (1998), using a thermally stimulated exoelectron emission dosimeter made of BeO, measured 62, 73 or 55-fold dose increases at the interface of a 150 μm thick gold sheet and a polymethylacrylate (PMMA, Plexiglas) plate irradiated with heavily filtered x-ray beams with 65, 85 or 100 keV mean energy, respectively. In addition, using the 65 keV beam, they found that the dose enhancement factor decreased exponentially with increasing distance from the Au-PMMA interface up to the maximum studied distance of 24 μm. Biological effects using a monolayer of cells were consistent with physical dosimetry. Similarly, Murthy and Lakshmanan (1976) measured a dose increase of ∼15 in PMMA using a 3 mg cm^{-2} thick thermoluminescent material in contact with a Au-PMMA interface and a 250 kVp x-ray beam filtered by 1 mm of Cu. In other words, the dose enhancement factor was higher with lower beam energies, consistent with our *in vivo* results.

For the actual animal gold biodistribution, the AuNPs are not uniformly distributed in the tumor, but are more concentrated at the tumor's growing edge, partly due to the reduced circulation at the tumor center and the leakiness of the angiogenic endothelium at the growing edge (Hainfeld *et al* 2004, 2010). Furthermore, for this and perhaps other subcutaneous tumor models, it appears that some extravasated gold may leak into the fascial plane between skin and muscle surrounding the tumor and be deposited too far away for tumor–dose enhancement.

Hyperthermia has long been known to synergize with RT (Kampinga 2006). There are several possible mechanisms to explain this phenomenon that are not mutually exclusive. Radiation is most effective with rapidly growing cells found mainly at the tumor periphery, whereas hypoxic cells with poor circulation, often found at the tumor interior, are relatively radiation-resistant. However, heat can damage tumor blood vessels and reduce tumor blood flow thereby exacerbating pre-existing hypoxia and kill the already malnourished hypoxic cells (Hinkelbein *et al* 1988). Combining these two modalities that affect complementary tumor cell populations can therefore have a dramatic synergistic effect as was seen in the study reported here. It is also possible that heat allows more gold to get into the tumor by enhancing the EPR effect (Friedl *et al* 2003) thereby increasing dose enhancement. There is also evidence that heating directly sensitizes hypoxic as well as euoxic cells to radiation. Heat is thought to change the physical properties of multiple protein cellular targets including cell membrane proteins that affect the integrity of the cell membrane and ultimately the redox status of cells leading to changes in the aggregation and associations of nuclear proteins which ultimately affect DNA repair and result in the amplification of DNA damage (Kampinga 2006, Roti Roti 2007, Roti Roti 2008, Vanderwaal *et al* 2009). The thermosensitivity of SCCVII has been described (Li *et al* 1992). Figure 4 and table 2 show the powerful synergy of ineffective moderate heating (44 °C for 20 min) and ineffective RT that, when combined, produced 100% cures (figure 4(C)). Since 44 °C for 20 min just prior to 30 Gy RT ablated all SCCVII tumors, one cannot assess an additional efficacy of AuNPs. By decreasing the RT to 15 Gy, the synergy of heat with RT is rendered far less dramatic. Now AuNPs are effective when either 23 Gy is used with a single fraction or 15 Gy is used with two fractions. These results are significant since the radiation dose can be drastically reduced when combined with gold and heat. The squamous cell carcinoma used here (SCCVII) is very radiation-resistant, with 50% of tumors being cured long-term (TCD50) by 55.4 Gy (Yahiro *et al* 2005), as are some human cancers

(Jones *et al* 2005). Importantly, with heat and gold, the same tumor control was achieved at 23 Gy (a radiation-dose reduction factor of 2.4). The combination of RT with heat and AuNPs is a powerful combination that warrants further development for clinical use.

Acknowledgments

We gratefully acknowledge Kerry Bonti, Renee Egusa, Michael Makar, Peggy Micca, Marta Nawrocky, Maryann Petry, and Mauro Testa for their help with various aspects of this study. JH is part owner of Nanoprobes, Inc. None of the remaining authors have any financial interest related to this work.

References

Adams F H, Norman A, Mello R S and Bass D 1977 Effect of radiation and contrast media on chromosomes. Preliminary report *Radiology* **124** 823–6

Argiris A, Karamouzis M V and Raben D 2008 Head and neck cancer *Lancet* **371** 1695–709

Bawarski W E, Chidlowsky E, Bharali D J and Mousa S A 2008 Emerging nanopharmaceuticals *Nanomedicine* **4** 273–82

Boisselier E and Astruc D 2009 Gold nanoparticles in nanomedicine: preparations, imaging, diagnostics, therapies and toxicity *Chem. Soc. Rev.* **38** 1759–82

Boudou C, Balosso J, Esteve F and Elleaume H 2005 Monte Carlo dosimetry for synchrotron stereotactic radiotherapy of brain tumors *Phys. Med. Biol.* **50** 4841–51

Browne E and Firestone R B 1986 *Table of Radioactive Isotopes* ed V Shirley (New York: Wiley)

Chapman D, Gmür N, Lazarz N and Thomlinson W 1988 Photon: a program for synchrotron radiation dose calculations *Nucl. Instrum. Meth.* A **266** 191–4

Cheng Y, Samia A C, Meyers J D, Panagopoulos I, Fei B and Burda C 2008 Highly efficient drug delivery with gold nanopaticle vectors for *in vivo* photodynamic therapy of cancer *J. Am. Chem. Soc.* **130** 10643–7

Cho S H 2005 Estimation of tumor dose enhancement due to gold nanoparticles during typical radiation treatments: a preliminary Monte Carlo study *Phys. Med. Biol.* **50** N163–73

Cho S H, Jones B L and Krishnan S 2009 The dosimetric feasibility of gold nanoparticle-aided radiation therapy (GNRT) via brachytherapy using low-energy gamma/x-ray sources *Phys. Med. Biol.* **54** 4889–905

Dilmanian F A, Morris G M, Zhong N, Bacarian T, Tammam J, Miura M, Micca P L, Rigon L, Scharf B, Slatkin D N, Yakupov R and Rosen E M 2001 Response of subcutaneous murine mammary carcinoma EMT-6 to synchrotron-generated segmented x-ray microbeams *Proc. of Joint Symp. on Bio-Sensing and Bio-Imaging* **1B-6** 118–22

Dilmanian F A, Morris G M, Zhong N, Bacarian T, Hainfeld J F, Kalef-Ezra J, Brewington L J, Tammam J and Rosen E M 2003 Murine EMT-6 carcinoma: high therapeutic efficacy of microbeam radiation therapy *Radiat. Res.* **159** 632–41

Dvorak H F 1990 Leaky tumor vessels: consequences for tumor stroma generation and for solid tumor therapy *Prog. Clin. Biol. Res.* **354A** 317–30

Friedl J, Turner E and Alexander H R Jr 2003 Augmentation of endothelial cell monolayer permeability by hyperthermia but not tumor necrosis factor: evidence for disruption of vascular integrity via VE-cadherin down-regulation *Int. J. Oncol.* **23** 611–6

Hainfeld J F, O'Connor M J, Dilmanian F A, Slatkin D N, Adams D J and Smilowitz H M 2010 MicroCT enables microlocalization and quantification of Her2-targeted gold nanoparticles within tumor regions *Br. J. Radiol.* (at press)

Hainfeld J F, Slatkin D N, Dilmanian F A and Smilowitz H M 2008 Radiotherapy enhancement with gold nanoparticles *J. Pharm. Pharmacol.* **60** 977–85

Hainfeld J F, Slatkin D N, Focella T and Smilowitz H M 2006 Gold nanoparticles as x ray contrast agents *Br. J. Radiol.* **79** 248–53

Hainfeld J F, Slatkin D N and Smilowitz H M 2004 Gold nanoparticles greatly enhance x-ray cancer therapy in mice *Phys. Med. Biol.* **49** N309–15

Herold D M, Das I J, Stobbe C C, Iyer R V and Chapman J D 2000 Gold microspheres: a selective technique for producing biologically effective dose enhancement *Int. J. Radiat. Biol.* **76** 1357–64

Hinkelbein W, Bruggmoser G, Engelhardt R and Wannemacher M 1988 *Preclinical Hyperthermia* (Berlin: Springer)

Hirsch L R, Gobin A M, Lowery A R, Tam F, Drezek R A, Halas N J and West J L 2006 Metal nanoshells *Ann. Biomed. Eng.* **34** 15–22

Ito S, Miyoshi N, Degraff W G, Nagashima K, Kirschenbaum L J and Riesz P 2009 Enhancement of 5-aminolevulinic acid-induced oxidative stress on two cancer cell lines by gold nanoparticles *Free Radic. Res.* **43** 121–4

Jones E L, Oleson J R, Prosnitz L R, Samulski T V, Vujaskovic Z, Yu D, Sanders L L and Dewhirst M W 2005 Randomized trial of hyperthermia and radiation for superficial tumors *J. Clin. Oncol.* **23** 3079–85

Kalef-Ezra J and Karava K 2008 Radiochromic film dosimetry: reflection versus transmission scanning *Med. Phys.* **35** 2308–11

Kampinga H H 2006 Cell biological effects of hyperthermia alone or combined with radiation or drugs: a short introduction to newcomers in the field *Int. J. Hyperthermia* **22** 191–6

Kinuya S, Yokoyama K, Hiramatsu T, Konishi S, Watanabe N, Shuke N, Aburano T, Bunko H, Michigishi T and Tonami N 2000 Optimal timing of administration of hyperthermia in combined radioimmunotherapy *Cancer Biother. Radiopharm.* **15** 373–9

Kong T, Zeng J, Wang X, Yang X, Yang J, McQuarrie S, McEwan A, Roa W, Chen J and Xing J Z 2008 Enhancement of radiation cytotoxicity in breast-cancer cells by localized attachment of gold nanoparticles *Small* **4** 1537–43

Lal S, Clare S E and Halas N J 2008 Nanoshell-enabled photothermal cancer therapy: impending clinical impact *Acc. Chem. Res.* **41** 1842–51

Lentner C 1982 *Geigy Scientific Tables* vol 2 8th edn (Basle: Geigy)

Li X, Brown SL and Hill R P 1992 Factors influencing the thermosensitivity of two rodent tumors *Radiat. Res.* **130** 211–9

Matsudaira H, Ueno A M and Furuno I 1980 Iodine contrast medium sensitizes cultured mammalian cells to x-rays but not to gamma rays *Radiat. Res.* **84** 144–8

McMahon S J, Mendenhall M H, Jain S and Currell F 2008 Radiotherapy in the presence of contrast agents: a general figure of merit and its application to gold nanoparticles *Phys. Med. Biol.* **53** 5635–51

Montenegro M, Nahar S N, Pradhan A K, Huang K and Yu Y 2009 Monte Carlo simulations and atomic calculations for Auger processes in biomedical nanotheranostics *J. Phys. Chem.* A **113** 12364–7

Moore A, Marecose E, Bogdanov A Jr and Weissleder R 2000 Tumoral distribution of long-circulating dextran-coated iron oxide nanoparticles in a rodent model *Radiology* **214** 568–74

Murthy M S and Lakshmanan A R 1976 Dose enhancement due to backscattered secondary-electrons at the interface of two media *Radiat. Res.* **67** 215–23

Muthu M S and Singh S 2009 Targeted nanomedicines: effective treatment modalities for cancer, AIDS and brain disorders *Nanomedicine* **4** 105–18

Nath R, Bongiorni P and Rockwell S 1990 Iododeoxyuridine radiosensitization by low- and high-energy photons for brachytherapy dose rates *Radiat. Res.* **124** 249–58

Nomura T, Shibabara T, Katakura A, Matsubara S and Takano N 2006 Establishment of a murine model of bone invasion by oral squamous cell carcinoma *Oral Oncol.* **43** 257–62

O'Malley B W Jr, Cope K A, Johnson C S and Schwartz M R 1997 A new immunocompetent murine model for oral cancer *Arch. Otolaryngol. Head Neck Surg.* **123** 20–4

Rahman W N, Bishara N, Ackerly T, He C F, Jackson P, Wong C, Davidson R and Geso M 2009 Enhancement of radiation effects by gold nanoparticles for superficial radiation therapy *Nanomedicine* **5** 136–42

Regulla D F, Hieber L B and Seidenbusch M 1998 Physical and biological interface dose effects in tissue due to x-ray-induced release of secondary radiation from metallic gold surfaces *Radiat. Res.* **150** 92–100

Roa W *et al* 2009 Gold nanoparticle sensitize radiotherapy of prostate cancer cells by regulation of the cell cycle *Nanotechnology* **20** 375101

Roeske J C, Nunez L, Hoggarth M, Labay E and Weichselbaum R R 2007 Characterization of the theoretical radiation dose enhancement from nanoparticles *Technol. Cancer Res. Treat.* **6** 395–402

Rose J H, Norman A, Ingram M, Aoki C, Solberg T and Mesa A 1999 First radiotherapy of human metastatic brain tumors delivered by a computerized tomography scanner (CTRx) *Int. J. Radiat. Oncol. Biol. Phys.* **45** 1127–32

Roti Roti J L 2007 Heat-induced alterations of nuclear protein associations and their effects on DNA repair and replication *Int. J. Hyperthermia* **23** 3–15

Roti Roti J L 2008 Cellular responses to hyperthermia (40–46 °C): cell killing an molecular events *Int. J. Hyperthermia* **24** 3–15

Serizawa T 2009 Radiosurgery for metastatic brain tumors *Int. J. Clin. Oncol.* **14** 289–98

Skrabalak S E, Au L, Lu X, Li X and Xia Y 2007 Gold nanocages for cancer detection and treatment *Nanomedicine* **2** 657–68

Vanderwaal R P, Maggi L B Jr, Weber J D, Hunt C R and Roti Roti J L 2009 Nucleophosmin redistribution following heat shock: a role in heat-induced radiosensitization *Cancer Res.* **69** 6454–62

Viani G A, Manta G B, Stefano E J and de Fendi L I 2009 Brachytherapy for cervix cancer: low-dose rate or high-dose rate brachytherapy—a meta-analysis of clinical trials *J. Exp. Clin. Cancer Res.* **28** 47–59

Wilkins R C, Ng C E and Raaphorst G P 1998 Comparison of high dose rate, low dose rate, and high dose rate fractionated radiation for optimizing differences in radiosensitivities *in vitro Radiat. Oncol. Invest.* **6** 209–15

Yahiro T, Masui S, Kubota N, Yamada K, Kobayashi A and Kishii K 2005 Effects of hypoxic cell radiosensitizer doranidazole (PR-350) on the radioresponse of murine and human tumor cells *in vitro J. Radiat. Res.* **46** 363–72

Yang D-P and Cui D-X 2008 Advances and prospects of gold nanorods *Chem. Asian J.* **3** 2010–22

Yang Y S, Guccione S and Bednarski M D 2003 Comparing genomic and histologic correlations to radiographic changes in tumors: a murine SCC VII model study *Acad. Radiol.* **10** 1165–75

Zhang S X, Gao J, Buchholz T A, Wang Z, Salehpour M R, Drezek R A and Yu T K 2009 *Biomed. Microdevices* **11** 925–33

Zheng Y and Sanche L 2009 Gold nanoparticles enhance DNA damage induced by anti-cancer drugs and radiation *Radiat. Res.* **172** 114–9